

1 **Both phenotypic and genotypic sex influence sex chromosome dosage**  
2 **compensation in a sex reversing lizard**

3

4 Benjamin J. Hanrahan<sup>1</sup>, J King Chang<sup>1</sup>, Nicholas C. Lister<sup>1</sup>, Duminda S.B.  
5 Dissanayake<sup>2</sup>, Jillian M. Hammond<sup>3,4</sup>, Andre L.M. Reis<sup>3,4,5</sup>, Ira W. Deveson<sup>3,4,5</sup>,  
6 Aurora Ruiz-Herrera<sup>6,7</sup>, Hardip R. Patel<sup>8</sup>, Jennifer A. Marshall Graves<sup>2,9</sup>, Arthur  
7 Georges<sup>2</sup>, Paul D. Waters<sup>1</sup>

8

9 <sup>1</sup> School of Biotechnology and Biomolecular Sciences, Faculty of Science, UNSW  
10 Sydney, Sydney, NSW 2052, Australia.

11 <sup>2</sup> Institute for Applied Ecology, University of Canberra, Canberra, ACT 2601  
12 Australia.

13 <sup>3</sup> Genomics Pillar, Garvan Institute of Medical Research, Sydney, NSW, Australia.

14 <sup>4</sup> Centre for Population Genomics, Garvan Institute of Medical Research and  
15 Murdoch Children's Research Institute, Australia.

16 <sup>5</sup> Faculty of Medicine, University of New South Wales, Sydney, NSW, Australia.

17 <sup>6</sup> Departament de Biologia Cel·lular, Fisiologia i Immunologia, Universitat Autònoma  
18 de Barcelona, Cerdanyola del Vallès, 08193, Spain.

19 <sup>7</sup> Genome Integrity and Instability Group, Institut de Biotecnologia i Biomedicina,  
20 Universitat Autònoma de Barcelona, Cerdanyola del Vallès, 08193, Spain.

21 <sup>8</sup> National Centre for Indigenous Genomics, Australian National University, ACT  
22 2601, Australia.

23 <sup>9</sup> Department of Environment and Genetics, La Trobe University, Melbourne, Victoria  
24 3068, Australia.

25

26

27 **Keywords:** sex chromosomes, dosage compensation, *Bassiana duperreyi*

28

29

30

31

32 **Abstract**

33

34 Studies of sex chromosome dosage compensation have historically focussed on  
35 therian mammals which have a conserved XY sex determination system. In contrast,  
36 lizards have sex determination systems that can differ between even closely related  
37 species that include XY and ZW systems and thermolabile systems where genetic  
38 and temperature interact to various degrees to determine sex. The eastern three-  
39 lined skink (*Bassiana duperreyi*) has a differentiated XY sex determination system, in  
40 which low temperature incubation during development can cause female to male sex  
41 reversal, producing XX males. This provides a unique opportunity to investigate how  
42 genotype and phenotype affect dosage compensation. We generated transcriptomes  
43 from brain and heart tissue of normal adult males and females, along with brain  
44 tissue of sex-reversed XX males. We observed partial dosage compensation  
45 between XX females and XY males in both brain and heart, with median gene  
46 expression from the X in normal males being 0.7 times that of normal females.  
47 Surprisingly, in brain of sex reversed XX males the median X chromosome output  
48 did not match that of either normal males or females, but instead was 0.89 times that  
49 of the normal XX female level. This suggests that not just genotype, but also sexual  
50 phenotype, influences gene dosage of the X chromosome. This has profound  
51 implications for our understanding of the evolution of dosage compensation.

52

53 **Introduction:**

54

55 Sex chromosome dosage compensation was proposed to have evolved in response  
56 to loss of gene function from the mammalian Y chromosome. Gene expression from  
57 the single X in males should need to be upregulated to restore ancestral autosomal  
58 levels. This X upregulation carried through to females resulting in disproportionately  
59 high X expression in XX females (1), and this was countered by X chromosome  
60 inactivation (XCI) to silence one X chromosome in the somatic cells of females (2).  
61 This classic model of dosage compensation appears to hold true for marsupial  
62 mammals, but transcriptional upregulation of the single X appears incomplete in  
63 eutherian mammals (3, 4). In monotremes, median gene expression from the X  
64 chromosome is increased compared to the autosomes in XY males, as it is for the  
65 bird Z in ZW females. However, global X (or Z) transcriptional output is not evenly  
66 balanced between the sexes (5).

67

68 Mammals and birds have ancient and relatively stable sex chromosomes and sex  
69 determination systems. Most mammals have a conserved XY system and birds have  
70 a conserved ZW system. In contrast, reptiles display a wide array of sex  
71 determination and sex chromosome systems, even in closely related species (6, 7).  
72 These organisms exhibit not only XY and ZW genetic sex determination (GSD)  
73 systems, but also temperature-dependent sex determination (TSD), whereby the sex  
74 of offspring is determined by the temperature at which the egg is incubated during a  
75 thermosensitive window. GSD and TSD systems are often observed in closely  
76 related lizard species, and some species have a GSD system that can be overridden  
77 by temperature to cause sex reversal (8-11).

78

79 The few studies of reptile dosage compensation have revealed a variety of non-  
80 canonical dosage compensation systems. In snakes, there are reports of partial  
81 dosage compensation of the Z chromosome by upregulation of Z-borne genes in  
82 females (12, 13). The green anole (*Anolis carolinensis*), a lizard with an XY sex  
83 chromosome system, has complete dosage compensation of genes on the linkage  
84 group representing the most differentiated region of the X, and incomplete dosage  
85 compensation of genes on scaffolds representing newer, less differentiated regions  
86 (14). In contrast, the Komodo dragon (*Varanus komodoensis*), which has one of the

87 oldest ZW sex chromosome systems, shows no evidence of dosage compensation  
88 of Z-specific genes (15). Little else is known about dosage compensation in other  
89 lizards with different sex chromosome systems.

90

91 The scincid lizard *Bassiana duperreyi* (Australian eastern three-lined skink) has a  
92 differentiated XY sex chromosome system (16) that is thought to predate skink  
93 radiation (17). However, the genetic sex determining switch can be overridden by  
94 temperature (8, 9, 11). Reduced incubation temperature of eggs during the  
95 thermosensitive period results in sex reversed XX males in the adult population and  
96 the natural nests of both captive and wild populations (18, 19). This gives rise to  
97 three different genotypic and phenotypic sexes: XX females, XY males and sex  
98 reversed XX males. Therefore, *B. duperreyi* provides a unique opportunity not only to  
99 examine dosage compensation in a reptile with differentiated sex chromosomes, but  
100 to also test if dosage compensation in sex reversed XX males follows genotype or  
101 phenotype.

102

103 Here we present a chromosome level *B. duperreyi* genome assembly from a male  
104 individual, in which we have identified both the X and Y chromosomes. We  
105 generated mRNA sequence data from brain and heart tissue of genotypically normal  
106 XX females and XY males, and brain tissue of XX male individuals to examine the  
107 effect of genotype and phenotype on dosage compensation. In brain and heart of  
108 normal XY male and XX female individuals, there was partial dosage compensation,  
109 such that the single X of XY males was overexpressed. However, in sex reversed XX  
110 males, we observed that median gene expression of the X was higher than in XY  
111 males, but lower than XX females, such that the X chromosomes of XX males were  
112 underexpressed. This raises the intriguing possibility that sex chromosome dosage  
113 compensation is not governed solely by genotype, and that phenotype (sex) plays an  
114 unknown role.

115

116

117

118

119

120 **Results:**

121

122 **Genome summary**

123 Genome length was 1.485 Gbp, assembled into 5,369 contigs/scaffolds. The six  
124 largest scaffolds corresponded to autosome macrochromosomes (288.7 - 75.5 Mbp),  
125 with the next eight largest scaffolds representing the microchromosomes (54.7 –  
126 18.1 Mbp) (Figure 1A, Table 1). These chromosome-scale scaffolds comprised  
127 98.5% of the total assembled sequence. BUSCO analysis showed 96.0% complete  
128 conserved orthologs in the tetrapod database and 96.6% complete conserved  
129 orthologs in the vertebrate database (Table 2).

130

131 **Table 1. Chromosome size and identity**

Scaffold Name	Size (bp)	Chromosome Identity
BASDU_flyeontv1_Contig31	288676622	1
BASDU_flyeontv1_Contig51	258390987	2
BASDU_flyeontv1_Contig32	215829809	3
BASDU_flyeontv1_Contig88	205722031	4
BASDU_flyeontv1_Contig66	107145552	5
BASDU_flyeontv1_Contig53	75523483	6
BASDU_flyeontv1_Contig1241	74033703	X
BASDU_flyeontv1_Contig298	54678650	7
BASDU_flyeontv1_Contig235	50055479	12,13,14
BASDU_flyeontv1_Contig328	39280427	8
BASDU_flyeontv1_Contig38	25948193	9
BASDU_flyeontv1_Contig604	22020833	10
BASDU_flyeontv1_Contig93	21659042	Y
BASDU_flyeontv1_Contig1096	18146980	11

132

133 **Table 2. BUSCO assessment of the *B. duperreyi* genome**

BUSCO Assessment	Total	Complete and single-copy	Complete and duplicated	Fragmented	Missing	Groups searched
<i>tetrapod_odb10</i>	5156	5098 (96.0%)	58 (1.1%)	44 (0.8%)	110 (2.1%)	38
<i>vertebrate_odb10</i>	3290	3240 (96.6%)	50 (1.5%)	32 (1.0%)	32 (0.9%)	67

134

135 Two scaffolds were identified as the X and Y chromosomes by BLASTn with known  
136 Y specific *B. duperreyi* markers. Read depth analysis of short read Illumina whole

137 genome sequencing from a male individual confirmed identity of these scaffolds as  
138 the X and Y chromosomes (Figure 1B), and revealed the pseudoautosomal region  
139 (PAR) boundary location at which read coverage increased compared to X and Y  
140 specific regions. The X and Y chromosomes were 71.2 Mbp and 21.7 Mbp,  
141 respectively, and shared a small PAR of approximately 2.8Mbp that was assembled  
142 onto the X scaffold (Figure 1B). Both the X and Y had more interactions with the  
143 autosomes, than macrochromosome to macrochromosome interactions (Figure 1A),  
144 contrasting eutherian XY systems that have fewer interactions between sex  
145 chromosome and autosomes (20). As expected, microchromosomes interacted with  
146 each other more than with the macrochromosomes (21).

147

148 Annotation identified a total of 13,979 genes in the genome. Of these, 667 were X-  
149 specific genes, sharing extensive homology with chicken chromosome 1 (Figure 1C).  
150 A total of 65 genes were annotated on the male specific region of the Y: 42 of these  
151 were X/Y shared, with the remaining 23 having no X-borne partner so were Y-  
152 specific. A total of 39 genes were annotated in the PAR. The karyotypic difference  
153 between the X and Y (16), and the disparity between their gene content, confirmed  
154 their differentiation. This suggested that a sex chromosome dosage compensation  
155 mechanism should be required to balance the output of X-specific genes in XX  
156 females and XY males.

157

### 158 **Dosage compensation of the X chromosome**

159 In brain and heart, median gene expression from the autosome scaffolds and PAR  
160 was equivalent between XY males and XX females (Figure 2A). However, median X  
161 chromosome transcriptional output in XY males was reduced compared to XX  
162 females (to 70% in brain and 65% in heart: Mood's median test,  $p < 0.0001$ ).

163

164 We next tested if phenotypic sex influenced total transcriptional output from the X  
165 versus the autosomes in brain. The ratios of median X specific to autosome gene  
166 expression levels within the three genotypic and phenotypic sexes were measured.  
167 In XX females there was no significant difference between X and autosomal  
168 expression levels. In XX males, expression from the X trended down, but this was  
169 not statistically significant. In XY males, median transcriptional output from the X was  
170 72% that of the autosomes (permutation test,  $p < 0.0001$ ) (Figure 2B).

171

172 We then compared transcriptional output of the X specific region between the three  
173 phenotypic and genotypic sexes. Median gene expression from autosome scaffolds  
174 and the PAR of XX females, XY males and sex reversed XX males were equivalent  
175 (Figure 2C). As observed for heart and brain above, median gene expression from  
176 the X chromosome was significantly lower in normal XY males compared to XX  
177 females (down to 69%: Mood's median test,  $p < 0.0001$ ) (Figure 2C). Median gene  
178 expression from the X chromosome was also lower in XY males than XX males  
179 (down to 77%: Mood's median test,  $p < 0.0001$ ). These ratios are both greater than  
180 the 50% expected from the dosage of X chromosomes, implying significant  
181 upregulation of the single X in XY males relative to XX females and XX males  
182 (Figure 2C).

183

184 The most interesting comparison of expression ratio from the X was between sex  
185 reversed XX males and normal XX females. Although both have two X  
186 chromosomes, transcription from the X was significantly lower in XX sex reversed  
187 males (down to 89%: Mood's median test,  $p < 0.0001$ ). This must mean that one or  
188 both X chromosomes are downregulated in sex reversed XX males. Thus, sex  
189 reversed XX males have a median level of X chromosome gene expression that is  
190 not equivalent to either their phenotypic (XY male) or genotypic (XX female)  
191 counterparts. This result is not region specific on the X (Figure 2D), nor is it restricted  
192 to a subset of genes (Figure 2G); rather, it is chromosome wide.

193

194

195 **Discussion:**

196

197 Therian mammals have conserved sex chromosomes and dosage compensation  
198 systems. Part of this dosage compensation system is the transcriptional silencing of  
199 one X in the somatic cells of females via the epigenetic process of XCI (2). In XXX  
200 human females, two Xs are inactivated (22), and in XXY males one X is silenced,  
201 leaving one active X (23, 24). This is a reflection of the counting mechanism of XCI,  
202 which results in all but one X being silenced in mammals (25) and is entirely  
203 genotype dependent.

204

205 In contrast, we demonstrate here that in a lizard transcriptional output of genes on  
206 the X chromosome is influenced by phenotypic sex, as well as sex chromosome  
207 constitution.

208

209 In normal XY male *B. duperreyi* there was partial dosage compensation of the X  
210 chromosome (Figure 2C), with median X chromosome gene expression 69% that of  
211 XX females. Therefore, the single X chromosome is being over-expressed by a  
212 factor of approximately 1.45. This is similar to observations in non-therian mammal  
213 vertebrates such as platypus (5). However, it is different from dosage compensation  
214 in other lizard species: absence of sex chromosome dosage compensation in the  
215 ZW system of the Komodo dragon (15), and a mix of complete and partial dosage  
216 compensation present in the green anole depending on the age of the region of the  
217 X chromosome (14).

218

219 Thus, our observation that *B. duperreyi* has a chromosome-wide partial dosage  
220 compensation system documents a third dosage compensation strategy in lizards.  
221 This implies that different dosage compensation systems have evolved repeatedly  
222 and independently in different lizard lineages, perhaps depending on the dosage  
223 compensation requirements of the progenitor autosomes from which the sex  
224 chromosome systems evolved. Study of more lizards will elucidate the breadth of  
225 reptile sex dosage compensation and highlight different evolutionary strategies.

226

227 As well as comparing normal XY males and XX females, we examined X expression  
228 in sex reversed XX males. Surprisingly, XX males had lower gene expression from



229 the X when compared to normal XX females, meaning that the expression per X is  
230 less in XX males than in XX females. Per X expression in XX males must also be  
231 less than expression from the single X in XY males (Figure 3). Therefore, sex  
232 chromosome dosage compensation in *B. duperreyi* is influenced not just by  
233 genotype, but also by sexual phenotype. This unexpected result is the first example  
234 of an effect of phenotype on sex chromosome dosage compensation, which has  
235 been viewed as a response strictly to genotype.

236

237 Reduced expression from the X in sex reversed XX males contradicts theories that  
238 dosage compensation evolves exclusively in response to genotype, that is to the  
239 number of X chromosomes. This is the first evidence that phenotypic sex influences  
240 sex chromosome transcriptional output, with profound implications for our  
241 understanding of how dosage compensation evolves. The underlying mechanism  
242 responsible for the effect of phenotypic sex on X gene expression remains unclear.  
243 Our observation suggests that there is down regulation of one or both of the Xs in XX  
244 males. This is quite the opposite to upregulation of the single X in XY males (Figure  
245 3).

246

247 Evolutionary arguments do not offer a satisfactory explanation of our results. If loss  
248 of genes from the degenerating Y was not accompanied by dosage compensation,  
249 we would expect expression from the two X chromosomes to be equivalent in XX  
250 females and XX sex reversed males. If loss of Y genes was accompanied by  
251 upregulation of the single X in XY males (which we observed), and upregulation of  
252 both Xs also occurred in XX males, we would expect XX males to have increased  
253 expression per X chromosome compared to XX females. Alternatively, should the X  
254 chromosomes in XX males have the same output as XX females, then XX males and  
255 XX females should be equivalent (Figure 3). None of these scenarios explain why  
256 expression from the X chromosome is lower in XX males than in XX females. Clearly  
257 X chromosome transcriptional output is not entirely a response to the number of X  
258 chromosomes. Therefore, we hypothesize that dosage compensation in *B. duperreyi*  
259 is influenced by phenotypic sex.

260

261 A possible explanation is that transcriptional output of the X in *B. duperreyi* is tuned  
262 to be globally lower in males than in females. This would not violate upregulation of

263 the single X in XY males in response to loss of genes from the Y, which results in the  
264 observed partial sex chromosome dosage compensation. However, if reduced  
265 expression from the X is optimal for normal males, then X output might be “capped”  
266 in phenotypic males irrespective of the number of X chromosomes. There is no  
267 subset of X-borne genes that is under expressed, so our results signify a global  
268 change in X expression (Figure 2 D-G). Understanding the epigenetic profile of the X  
269 chromosomes in the three genotypic and phenotypic sexes will be critical to  
270 deciphering the mechanics of dosage compensation in this model.

271

272 Temperature-induced sex reversal in lizards is not unique to *B. duperreyi*, having  
273 been observed in several species (8, 10). It is possible that sex reversal in lizards is  
274 more widespread than previously believed, as it has been systematically investigated  
275 in only a few species (26), and there may be numerous other species whose sex  
276 reversal status is yet to be confirmed (see 27, 28, 29). Examining dosage  
277 compensation in other sex reversing models will reveal if the influence that  
278 phenotypic sex exerts on X (or Z) gene expression is a widespread phenomenon in  
279 lizards.

280

281 **Methods**

282

283 **Sample collection and sexing**

284 In December 2020, samples (eggs) of alpine *B. duperreyi* were collected from the  
285 field location within the Brindabella Range (Piccadilly Circus – 1240 m a.s.l.,  
286 35°21'42.0"S 148°48'12.5"E) after ensuring that approximately 90% of the  
287 development period had passed in natural conditions (9). The eggs were then  
288 collected, transported to the University of Canberra, and placed in incubators  
289 (LabWit, ZXSDR1090) that maintained 23°C, which produces a balanced sex ratio  
290 (9). Details egg collection methods (19) and a description of the alpine study site can  
291 be found in (30).

292

293 To determine phenotypic sex of the hatchlings, tail bases of 3-to-7-day old hatchlings  
294 were squeezed to evert the hemipenes (31) and sex was checked again by  
295 hemipene transillumination after 5 weeks (19). Tail snips were collected to determine  
296 the genotype of the lizards. Genotypic sex was determined for *B. duperreyi* using  
297 polymerase chain reaction (PCR)-based molecular sex tests from extracted DNA  
298 collected from tissue samples. DNA purity was determined using a NanoDrop 1000  
299 spectrophotometer (NanoDrop Technologies Inc., Wilmington, DE, USA) and  
300 quantified using the Qubit 2.0 Fluorometric Quantitation (Invitrogen, Life  
301 technologies, Sydney, N.S.W., Australia). The sex-reversal status was determined  
302 for *B. duperreyi* using PCR as described by Dissanayake et al. (16), where the  
303 genotypic sex was identified based on Y-specific markers allowing identification of  
304 XY males (XYm) and XX males (XXm).

305

306

307 **RNA extraction and sequencing**

308 Total RNA was extracted from the brain tissue of five XY males (XYm), five XX  
309 females (XXfm), and four XX males (XXm). Tissue extracts were homogenized using  
310 T10 Basic ULTRA-TURRAX® Homogenizer (IKA, Staufen im Breisgau, Germany)  
311 and extracted using TRIzol reagent following the manufacturer's instructions,  
312 purifying with an isopropanol precipitation. Seventy-five bp single-ended reads were  
313 generated on the Illumina NextSeq 500 platform at the Ramaciotti Centre for  
314 Genomics (UNSW, Sydney, Australia).

315

316

### 317 **DNA extraction and sequencing for assembly**

318 Genomic DNA was extracted from 13 mg of ethanol-preserved muscle tissue from a  
319 male (XY) *B. duperreyi*, using the Circulomics Nanobind tissue kit as per the  
320 manufacturer's protocols, including the specified pre-treatment for ethanol removal.  
321 Library preparation was performed with 3 µg of DNA as input, using the SQK-  
322 LSK109 kit from Oxford Nanopore Technologies and sequenced across two  
323 promethION (FLO-PRO002) flow cells, with washes (EXP-WSH004) performed  
324 every 24 hours.

325

### 326 **Genome assembly**

327 The genome assembly pipeline relied on using a combination of whole-genome  
328 sequencing ONT long reads, Illumina short reads and Hi-C reads. Firstly, adapters  
329 were removed from Illumina and Hi-C reads using TrimGalore v0.6.6 with default  
330 parameters. A primary assembly was generated using Flye v2.8.3 (32) and the ONT  
331 long reads, with the following parameters "--trestle --iterations 2". Illumina short  
332 reads were aligned to the primary assembly with bwa-mem v0.7.17-r1188 and ONT  
333 long reads were aligned with minimap2 v2.24-r1122 (33), and both alignments were  
334 used to polish the assembly with hypo v0.5.1. Homologous contigs were identified  
335 and removed using Purge Haplotigs v1.1.1 (34). Chromosome-length scaffolding  
336 was performed with Hi-C data using Juicer v1.6 (35) to generate a contact matrix of  
337 the connections between contigs and 3d-dna v180922 to organise the contigs into  
338 larger scaffolds. Gaps in the assembly were filled using PBJelly v15.8.24 (36) with  
339 the ONT reads. The final assembly was assessed for completeness using BUSCO  
340 and accuracy using Merqury v1.3 (37), by comparing the assembly k-mer spectrum  
341 to those found in the Illumina reads.

342

### 343 **Annotation**

344 The annotation used in this study was generated using AUGUSTUS v3.4.0 (38) with  
345 RNA sequencing data from brain, heart and gonad from male and female individuals.  
346 Prior to running AUGUSTUS, a transcriptome assembly and a soft-masked genome  
347 assembly were generated with Trinity v2.12.0 (39) and RepeatMasker v4.1.2-p1  
348 (40), respectively. AUGUSTUS parameters were optimised with a training set of 500

349 genes, including 5 rounds of optimisation with exon and UTR parameters, before  
350 gene prediction and stitching. Peptides were inferred from the final annotation using  
351 gffread v0.12.7 (41) and blasted against the uniprot database with blast v2.11.0 (42)  
352 for gene identification. A github repository of this pipeline can be found at  
353 <https://github.com/kango2/Annotation>.

354

355 Y specific sequences (16) in *Bassiana* were blasted against the generated *Bassiana*  
356 *duperreyi* genome assembly with blast v2.11.0 (42).

357

### 358 **Read depth analysis**

359 DNA was extracted from muscle samples of the individual animals using the Gentra  
360 Puregene Tissue Kit (QIAGEN, Australia), following the manufacturer's protocols  
361 with the modifications described below. The volume and reagent amounts were  
362 adjusted according to the size of the tissue sample, using three times more reagent  
363 than specified in the manufacturer's protocols. Additionally, we made modifications  
364 to the DNA precipitation steps outlined in the manufacturer's protocol. The DNA  
365 thread was spooled out using a galls rod and submerged in 300ul of 70% ethanol,  
366 then air dried for one minute. Subsequently, we used TE buffer for DNA hydration  
367 and allowed it to dissolve overnight at room temperature.

368

369 Raw read quality of the DNA sequencing was assessed using FastQC v0.11.9 (43)  
370 and trimmed accordingly with trimmomatic v0.38 (44). Trimmed reads were aligned  
371 to the newly generated *B. duperreyi* genome assembly with subread-align command  
372 in subread v2.0.1 (45). Read depth in 20000 bp windows was calculated using the  
373 bamCoverage command, from deeptools v3.5.1 (46), for the X and Y scaffolds as  
374 well as a representative autosomal scaffold (contig 328). The generated BED files  
375 were then used to plot read depth across these scaffolds using the ggplot2 package  
376 in R v4.2.1.

377

### 378 **Bioinformatics analysis of RNA-seq**

379 Raw read quality of RNA sequencing was assessed using FastQC v0.11.9 (43) and  
380 trimmed accordingly with trimmomatic v0.38 (44). Trimmed reads were aligned to the  
381 newly generated *B. duperreyi* genome assembly with subread-align function in  
382 subread v2.0.1 (45). The subread-featurecount function from subread v2.0.1 (47)

383 was used to count reads that overlapped genomic features using the settings “-0 -2 -t  
384 CDS,five\_prime\_utr,three\_prime\_utr”, the remaining settings were left as default.  
385 Library size and read counts were normalised by counts per million and RPKM  
386 respectively using the edgeR package in R v4.2.1 (48). Gene expression ratios were  
387 calculated and plotted with the ggplot2 package. Gene expression values were  
388 calculated from the RNA-seq data (hatchling brain tissue) of XX females (n=3), XY  
389 males (n=3) and sex reversed XX males (n=3). Normalised expression values were  
390 used to create male to female median expression ratios between the three genotypic  
391 and phenotypic sexes for each gene. Genes were binned according to their location  
392 on an autosome, the PAR, X as total output and X where output is adjusted for X  
393 complement. For per X median expression ratios, X expression was halved for the  
394 sexes with two X chromosomes (XXf and XXm).

395

#### 396 **Data availability**

397 All sequence data have been submitted to the NCBI sequence read archive under  
398 the BioProject ID PRJNA980841.

399 **References**

- 400 1. Ohno S. Sex chromosomes and sex-linked genes. Berlin, New York etc.:  
401 Springer-Verlag; 1967. x, 192 p. p.
- 402 2. Lyon MF. X-chromosome inactivation and developmental patterns in  
403 mammals. *Biol Rev Camb Philos Soc.* 1972;47(1):1-35.
- 404 3. Xiong Y, Chen X, Chen Z, Wang X, Shi S, Wang X, et al. RNA sequencing  
405 shows no dosage compensation of the active X-chromosome. *Nat Genet.*  
406 2010;42(12):1043-7.
- 407 4. Lin F, Xing K, Zhang J, He X. Expression reduction in mammalian X  
408 chromosome evolution refutes Ohno's hypothesis of dosage compensation. *Proc*  
409 *Natl Acad Sci U S A.* 2012;109(29):11752-7.
- 410 5. Julien P, Brawand D, Soumillon M, Necsulea A, Liechti A, Schutz F, et al.  
411 Mechanisms and evolutionary patterns of mammalian and avian dosage  
412 compensation. *PLoS Biol.* 2012;10(5):e1001328.
- 413 6. Sarre SD, Georges A, Quinn A. The ends of a continuum: genetic and  
414 temperature-dependent sex determination in reptiles. *Bioessays.* 2004;26(6):639-45.
- 415 7. Ezaz T, Sarre SD, O'Meally D, Graves JAM, Georges A. Sex chromosome  
416 evolution in lizards: independent origins and rapid transitions. *Cytogenet Genome*  
417 *Res.* 2009;127(2-4):249-60.
- 418 8. Quinn AE, Georges A, Sarre SD, Guarino F, Ezaz T, Graves JA. Temperature  
419 sex reversal implies sex gene dosage in a reptile. *Science.* 2007;316(5823):411.
- 420 9. Shine R, Elphick MJ, Donnellan S. Co-occurrence of multiple, supposedly  
421 incompatible modes of sex determination in a lizard population. *Ecol Lett.*  
422 2002;5(4):486-9.
- 423 10. Holleley CE, O'Meally D, Sarre SD, Graves JAM, Ezaz T, Matsubara K, et al.  
424 Sex reversal triggers the rapid transition from genetic to temperature-dependent sex.  
425 *Nature.* 2015;523(7558):79-82.
- 426 11. Radder RS, Quinn AE, Georges A, Sarre SD, Shine R. Genetic evidence for  
427 co-occurrence of chromosomal and thermal sex-determining systems in a lizard. *Biol*  
428 *Lett.* 2008;4(2):176-8.
- 429 12. Vicoso B, Emerson JJ, Zektser Y, Mahajan S, Bachtrog D. Comparative sex  
430 chromosome genomics in snakes: differentiation, evolutionary strata, and lack of  
431 global dosage compensation. *PLoS Biol.* 2013;11(8):e1001643.

- 432 13. Schield DR, Card DC, Hales NR, Perry BW, Pasquesi GM, Blackmon H, et al.  
433 The origins and evolution of chromosomes, dosage compensation, and mechanisms  
434 underlying venom regulation in snakes. *Genome Res.* 2019;29(4):590-601.
- 435 14. Rupp SM, Webster TH, Olney KC, Hutchins ED, Kusumi K, Wilson Sayres  
436 MA. Evolution of Dosage Compensation in *Anolis carolinensis*, a Reptile with XX/XY  
437 Chromosomal Sex Determination. *Genome Biol Evol.* 2017;9(1):231-40.
- 438 15. Rovatsos M, Rehak I, Velenský P, Kratochvil L. Shared Ancient Sex  
439 Chromosomes in Varanids, Beaded Lizards, and Alligator Lizards. *Mol Biol Evol.*  
440 2019;36(6):1113-20.
- 441 16. Dissanayake DSB, Holleley CE, Hill LK, O'Meally D, Deakin JE, Georges A.  
442 Identification of Y chromosome markers in the eastern three-lined skink (*Bassiana*  
443 *duperreyi*) using in silico whole genome subtraction. *BMC Genomics.*  
444 2020;21(1):667.
- 445 17. Kostmann A, Kratochvil L, Rovatsos M. Poorly differentiated XX/XY sex  
446 chromosomes are widely shared across skink radiation. *Proc Biol Sci.*  
447 2021;288(1943):20202139.
- 448 18. Dissanayake DSB, Holleley CE, Deakin JE, Georges A. High elevation  
449 increases the risk of Y chromosome loss in Alpine skink populations with sex  
450 reversal. *Heredity (Edinb).* 2021;126(5):805-16.
- 451 19. Dissanayake DSB, Holleley CE, Georges A. Effects of natural nest  
452 temperatures on sex reversal and sex ratios in an Australian alpine skink. *Sci Rep.*  
453 2021;11(1):20093.
- 454 20. Álvarez-González L, Arias-Sardá C, Montes-Espuña L, Marín-Gual L, Vara C,  
455 Lister NC, et al. Principles of 3D chromosome folding and evolutionary genome  
456 reshuffling in mammals. *Cell Rep.* 2022;41(12):111839.
- 457 21. Waters PD, Patel HR, Ruiz-Herrera A, Álvarez-González L, Lister NC,  
458 Simakov O, et al. Microchromosomes are building blocks of bird, reptile, and  
459 mammal chromosomes. *Proc Natl Acad Sci U S A.* 2021;118(45).
- 460 22. Nielsen MM, Trolle C, Vang S, Hornshøj H, Skakkebæk A, Hedegaard J, et al.  
461 Epigenetic and transcriptomic consequences of excess X-chromosome material in  
462 47,XXX syndrome-A comparison with Turner syndrome and 46,XX females. *Am J*  
463 *Med Genet C Semin Med Genet.* 2020;184(2):279-93.



- 464 23. Kinjo K, Yoshida T, Kobori Y, Okada H, Suzuki E, Ogata T, et al. Random X  
465 chromosome inactivation in patients with Klinefelter syndrome. *Mol Cell Pediatr.*  
466 2020;7(1):1.
- 467 24. Zitzmann M, Bongers R, Werler S, Bogdanova N, Wistuba J, Kliesch S, et al.  
468 Gene expression patterns in relation to the clinical phenotype in Klinefelter  
469 syndrome. *J Clin Endocrinol Metab.* 2015;100(3):E518-23.
- 470 25. Avner P, Heard E. X-chromosome inactivation: counting, choice and initiation.  
471 *Nat Rev Genet.* 2001;2(1):59-67.
- 472 26. Holleley CE, Sarre SD, O'Meally D, Georges A. Sex Reversal in Reptiles:  
473 Reproductive Oddity or Powerful Driver of Evolutionary Change? *Sex Dev.*  
474 2016;10(5-6):279-87.
- 475 27. Whiteley SL, Castelli MA, Dissanayake DSB, Holleley CE, Georges A.  
476 Temperature-Induced Sex Reversal in Reptiles: Prevalence, Discovery, and  
477 Evolutionary Implications. *Sex Dev.* 2021;15(1-3):148-56.
- 478 28. Cornejo-Páramo P, Dissanayake DSB, Lira-Noriega A, Martínez-Pacheco ML,  
479 Acosta A, Ramírez-Suástegui C, et al. Viviparous Reptile Regarded to Have  
480 Temperature-Dependent Sex Determination Has Old XY Chromosomes. *Genome*  
481 *Biol Evol.* 2020;12(6):924-30.
- 482 29. Van Dyke JU, Thompson MB, Burrige CP, Castelli MA, Clulow S,  
483 Dissanayake DSB, et al. Australian lizards are outstanding models for reproductive  
484 biology research. *Australian Journal of Zoology.* 2020;68(4):168-99.
- 485 30. Dissanayake DSB, Holleley CE, Sumner J, Melville J, Georges A. Lineage  
486 diversity within a widespread endemic Australian skink to better inform conservation  
487 in response to regional-scale disturbance. *Ecol Evol.* 2022;12(3):e8627.
- 488 31. Harlow PS. A Harmless Technique for Sexing Hatchling Lizards. *Herpetol*  
489 *Rev.* 1996;27(2):71-.
- 490 32. Kolmogorov M, Yuan J, Lin Y, Pevzner PA. Assembly of long, error-prone  
491 reads using repeat graphs. *Nat Biotechnol.* 2019;37(5):540-6.
- 492 33. Li H. Minimap2: pairwise alignment for nucleotide sequences. *Bioinformatics.*  
493 2018;34(18):3094-100.
- 494 34. Roach MJ, Schmidt SA, Borneman AR. Purge Haplotigs: allelic contig  
495 reassignment for third-gen diploid genome assemblies. *BMC Bioinformatics.*  
496 2018;19(1):460.

- 497 35. Durand NC, Shamim MS, Machol I, Rao SS, Huntley MH, Lander ES, et al.  
498 Juicer Provides a One-Click System for Analyzing Loop-Resolution Hi-C  
499 Experiments. *Cell Syst.* 2016;3(1):95-8.
- 500 36. English AC, Richards S, Han Y, Wang M, Vee V, Qu J, et al. Mind the gap:  
501 upgrading genomes with Pacific Biosciences RS long-read sequencing technology.  
502 *PLoS One.* 2012;7(11):e47768.
- 503 37. Rhie A, Walenz BP, Koren S, Phillippy AM. Merqury: reference-free quality,  
504 completeness, and phasing assessment for genome assemblies. *Genome Biol.*  
505 2020;21(1):245.
- 506 38. Stanke M, Diekhans M, Baertsch R, Haussler D. Using native and syntenically  
507 mapped cDNA alignments to improve de novo gene finding. *Bioinformatics.*  
508 2008;24(5):637-44.
- 509 39. Grabherr MG, Haas BJ, Yassour M, Levin JZ, Thompson DA, Amit I, et al.  
510 Full-length transcriptome assembly from RNA-Seq data without a reference genome.  
511 *Nat Biotechnol.* 2011;29(7):644-52.
- 512 40. Smit AFA, Hubley R, Green P. RepeatMasker Open-4.0. 2013-2015.
- 513 41. Perteza G, Perteza M. GFF Utilities: GffRead and GffCompare. *F1000Res.*  
514 2020;9.
- 515 42. Camacho C, Coulouris G, Avagyan V, Ma N, Papadopoulos J, Bealer K, et al.  
516 BLAST+: architecture and applications. *BMC Bioinformatics.* 2009;10:421.
- 517 43. Andrews S. FastQC: a quality control tool for high throughput sequence data.  
518 2010.
- 519 44. Bolger AM, Lohse M, Usadel B. Trimmomatic: a flexible trimmer for Illumina  
520 sequence data. *Bioinformatics.* 2014;30(15):2114-20.
- 521 45. Liao Y, Smyth GK, Shi W. The Subread aligner: fast, accurate and scalable  
522 read mapping by seed-and-vote. *Nucleic Acids Res.* 2013;41(10):e108.
- 523 46. Ramirez F, Ryan DP, Gruning B, Bhardwaj V, Kilpert F, Richter AS, et al.  
524 deepTools2: a next generation web server for deep-sequencing data analysis.  
525 *Nucleic Acids Res.* 2016;44(W1):W160-5.
- 526 47. Liao Y, Smyth GK, Shi W. featureCounts: an efficient general purpose  
527 program for assigning sequence reads to genomic features. *Bioinformatics.*  
528 2014;30(7):923-30.

- 529 48. Robinson MD, McCarthy DJ, Smyth GK. edgeR: a Bioconductor package for  
530 differential expression analysis of digital gene expression data. *Bioinformatics*.  
531 2010;26(1):139-40.
- 532 49. Ramirez F, Bhardwaj V, Arrigoni L, Lam KC, Gruning BA, Villaveces J, et al.  
533 High-resolution TADs reveal DNA sequences underlying genome organization in  
534 flies. *Nat Commun*. 2018;9(1):189.
- 535 50. Lovell JT, Sreedasyam A, Schranz ME, Wilson M, Carlson JW, Harkess A, et  
536 al. GENESPACE tracks regions of interest and gene copy number variation across  
537 multiple genomes. *Elife*. 2022;11.
- 538

539 **Figure Legends**

540

541 **Figure 1. Genome summary of the *Bassiana duperreyi* assembly**

542 **A)** Hi-C contact map generated with HiC explorer (49) showing scaffold  
543 (chromosome) boundaries. Inset: magnified view of the HiC contact map for  
544 microchromosomes with size 18.1 – 55.4 Mb, and the sex chromosomes. Number of  
545 contacts are between 100 kbp bins. Below: mean inter-chromosomal interactions for  
546 100 kbp windows between each chromosome. **B)** Number of reads mapped in 20kb  
547 windows of male Illumina genome sequencing on a representative autosome (contig  
548 31), the putative Y (contig 93) and X contigs (contig 1241). Vertical red line is the  
549 PAR boundary on the X contig. **C)** Synteny across chicken, bassiana and blue tailed  
550 skink (*Cryptoblepharus egeriae*) genomes, generated with GENESPACE (50). The  
551 bassiana Y scaffold (contig 93, not shown) does not share synteny with the other two  
552 species.

553

554 **Figure 2. Dosage of gene expression between sexes**

555 **A)** Median expression male (XY) to female (XX) ratios were calculated for brain and  
556 heart tissue (n=1 for both). A ratio above zero indicates higher expression in male  
557 and a ratio below zero indicates higher expression in female. Median is plotted in the  
558 box with exact value above each median. Boxes represent the middle 50% of the  
559 data, and whiskers represent 1.5 times the interquartile range. Outliers not plotted.  
560 **B)** Brain transcriptomes were used to calculate median RPKM for each sex condition  
561 (XYm, XXm and XXf) and plotted for autosomal, X specific and PAR genes as a ratio  
562 to autosomal median. Ratio to the autosomal median is plotted in the box with exact  
563 value above each median. Permutation tests were used to calculate whether median  
564 PAR and X specific RPKMs were statistically different from the median autosome  
565 RPKM, as well as if the median PAR RPKM was different from the median X specific  
566 RPKM (\*\*\*\* p<0.0001, \*\*\* p<0.001, \* p<0.05). **C)** Median expression ratios were  
567 calculated for pairwise comparisons of the three sexes (XYm, XXm and XXf).  
568 Genomic regions were separated and plotted as follows; autosomes (green), PAR  
569 (blue), total X output (red) and X output adjusted per X (yellow). Mood's median tests  
570 were used to calculate if the ratios for the autosomes and X, as well as Xs between  
571 sexes, were statistically different (\*\*\*\* p<0.0001). **D)** Expression ratios were  
572 calculated for each gene in the X specific region and PAR in a pairwise fashion for

573 the three sexes. Ratios plotted on a log<sub>2</sub> scale and median values are plotted as a  
574 line in red for X the specific region and blue for the PAR. **E-G**) Scatterplot of counts  
575 per million (CPM) for each gene for each pairwise comparison of **E**) XXf to XYm, **F**)  
576 XXm to XYm and **G**) XXf to XXm. X genes are plotted in black with slope plotted as a  
577 red line. Autosomal genes are plotted in blue with slope as a green line. Slope and  
578 R-squared of each trendline is shown above each plot.

579

580 **Figure 3. Expected and observed dosage of the X chromosome in sex reversed**

581 **XX males.** Left: The X chromosome must be upregulated to in XY males to reach  
582 ~70% of the total X chromosome transcriptional output in females. Centre: Should  
583 dosage compensation depend on genotype, then transcriptional output of the X  
584 chromosomes in XX males should be the same as XX females (top). Alternatively, if  
585 transcriptional output of the X chromosome depends on phenotype, then both X  
586 chromosomes should be up regulated (bottom) resulting in total X output greater  
587 than that of XX females. Right: The total transcriptional output from X genes in XX  
588 males lay between that of XX females and XY male. This could result from an  
589 upregulated X (as in XY males) that is coupled with a mostly down-regulated X (top).  
590 Alternatively, two partially down-regulated Xs (bottom) could achieve the same  
591 transcriptional output.

592

593 **Supplementary Figure 1.** Expression ratios for each autosomal scaffold for the  
594 three pairwise sex/ genotype comparisons. Number of genes (n) is show in the key  
595 for each contig.

596

597 **Supplementary Figure 2.** Expression ratios were calculated for each gene on a  
598 representative autosome in a pairwise fashion for each sex (XYm, XXm and XXf).  
599 Values are plotted on a log<sub>2</sub> scale and median values for each comparison are  
600 plotted as a red line.

601

602 **Acknowledgements**

603 Sequencing costs for this project were met by grants from Bioplatforms Australia  
604 (AusARG initiative) and the Australian Research Council (DP170101147). We  
605 acknowledge the Garvan Sequencing Platform.

606

607 **Funding**

608 P.D.W. and J.A.M. are supported by Australian Research Council Discovery Projects  
609 (DP170101147, DP180100931, DP210103512 and DP220101429). P.D.W. and  
610 H.R.P. are supported by an NHMRC Ideas Grant (2021172). A.R.-H. acknowledges  
611 the Spanish Ministry of Science and Innovation (PID2020-112557GB-I00) and the  
612 Agència de Gestió d'Ajuts Universitaris i de Recerca, AGAUR (2021SGR00122).

613

614 **Competing interests**

615 The authors declare that they have no competing interests.

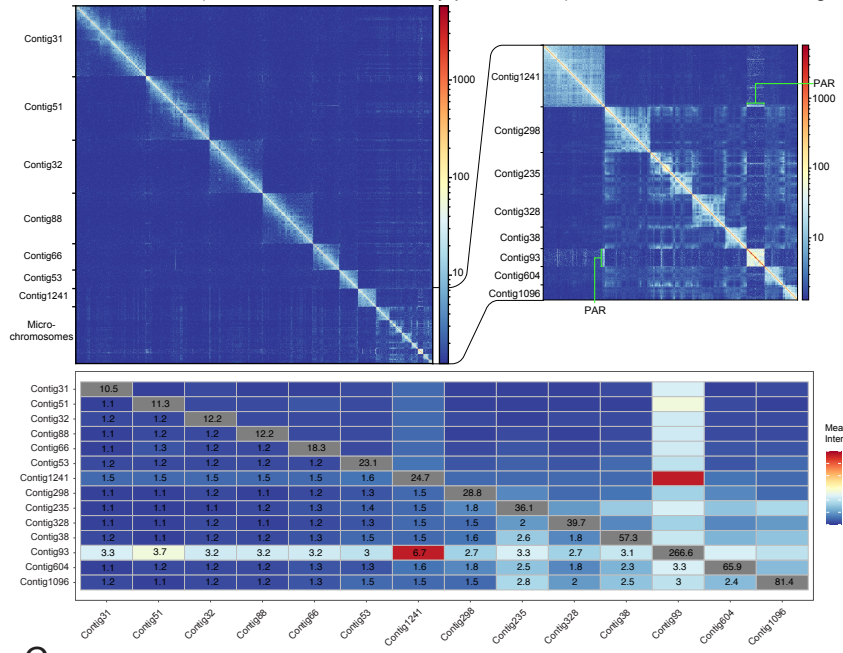
616

617 **Ethics approval**

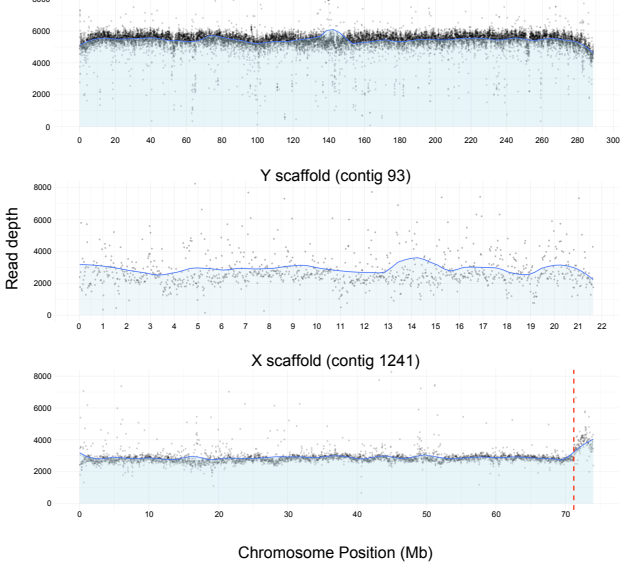
618 Experimentation using animals was approved by the University of Canberra Animal  
619 Ethics Committee (AEC 17–26) and NSW (SL102002) and ACT (LT201826,  
620 LT2017956) governments granted research permits. Husbandry practices fulfil the  
621 Australian Code for the Care and Use of Animals for Scientific Purposes 8th edition  
622 (2013) sections 3.2.13–3.2.2.

623

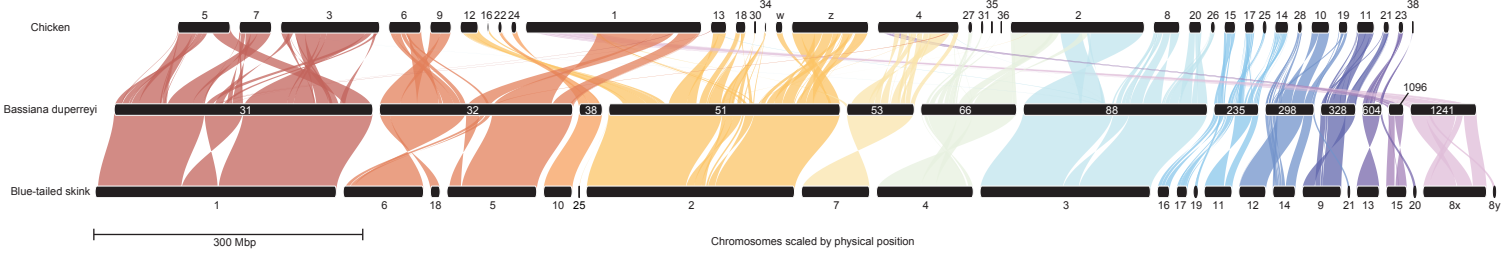
A



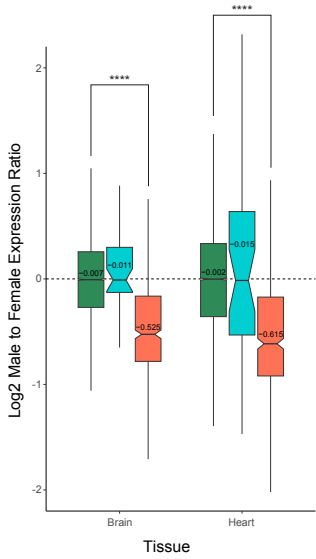
B



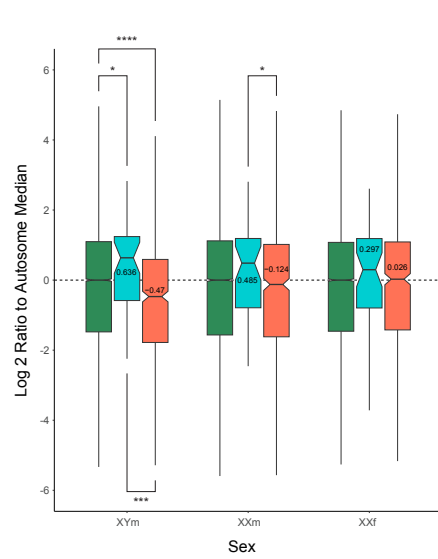
C



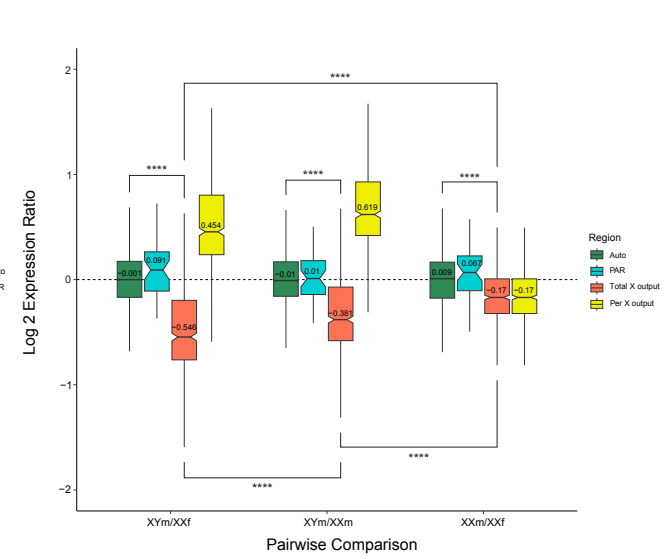
A



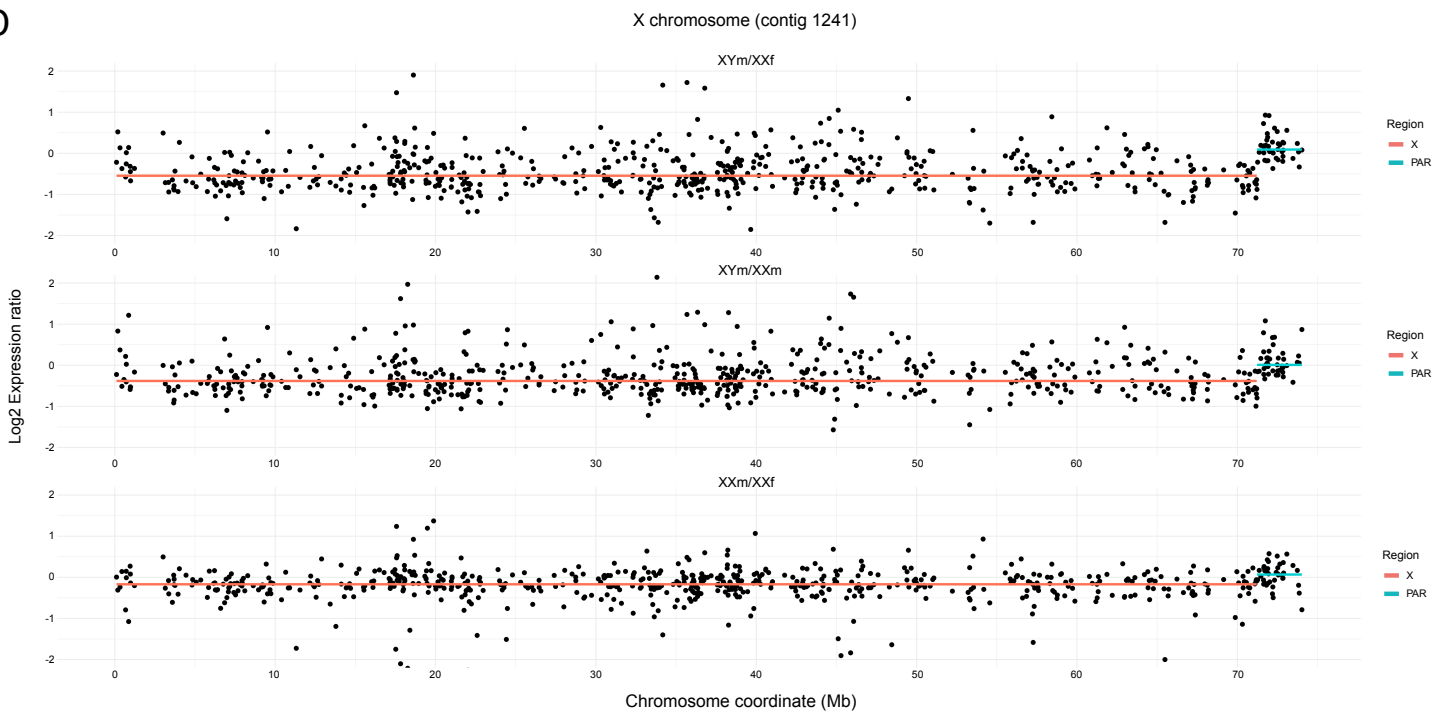
B



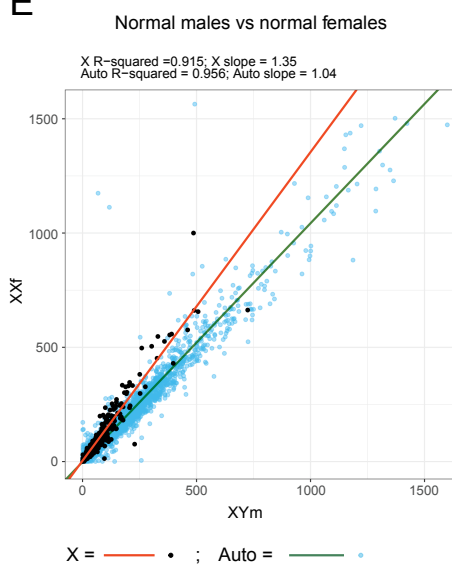
C



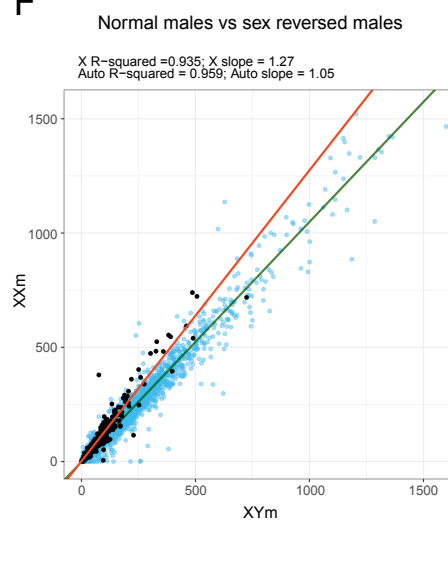
D



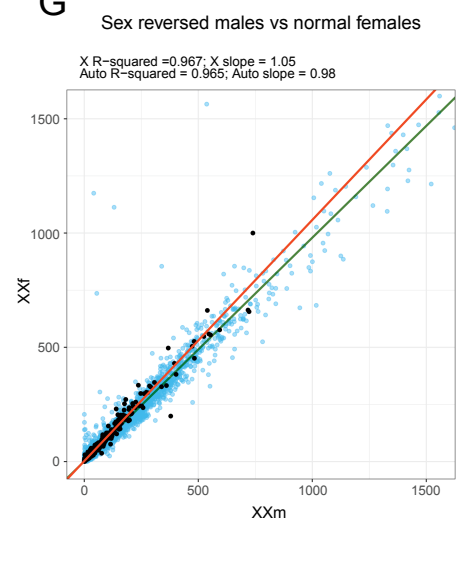
E



F



G



X = —•— ; Auto = —•—



